Anisotropic relaxation and crystallographic tilt in $BiFeO_3$ on miscut $SrTiO_3$ (001)

Rebecca J. Sichel,[1] Alexei Grigoriev,[1,a)] Dal-Hyun Do,[1] Seung-Hyub Baek,[1] Ho-Won Jang,[1] Chad M. Folkman,[1] Chang-Beom Eom,[1] Zhonghou Cai,[2] and Paul G. Evans[1,b)]

[1]*Materials Science Program, University of Wisconsin, Madison, Wisconsin 53706, USA*
[2]*Advanced Photon Source, Argonne National Laboratory, Argonne, Illinois 60439, USA*

(Received 25 October 2009; accepted 6 January 2010; published online 1 February 2010)

Epitaxial $BiFeO_3$ thin films on miscut (001) $SrTiO_3$ substrates relax via mechanisms leading to an average rotation of the crystallographic axes of the $BiFeO_3$ layer with respect to the substrate. The angle of the rotation reaches a maximum in the plane defined by the surface normal of the film and the direction of the surface miscut. X-ray microdiffraction images show that each $BiFeO_3$ mosaic block is rotated by a slightly different angle and contains multiple polarization domains. These effects lead to a complicated overall symmetry in $BiFeO_3$ thin films. This relaxation mechanism can be extended to other complex oxides. © *2010 American Institute of Physics*.
[doi:10.1063/1.3299256]

The relaxation of stresses arising from the lattice mismatch in heteroepitaxy influences the functional properties of resulting structures and defines much of the scientific challenge of epitaxial growth. The piezoelectricity and ferroelectric domain structure of ferroelectric and multiferroic oxides can be modified by epitaxial stresses, which distort the crystallographic unit cell, and in extreme cases can lead to changes in the structural phase.[1,2] The relaxation of stress and its influence on the resulting structure of complex heterostructures involving materials of different crystallographic symmetries is particularly challenging. $BiFeO_3$, for example, is a rhombohedrally distorted perovskite with a pseudocubic bulk lattice constant of 3.96 Å that is often grown as a thin film on cubic substrates such as $SrTiO_3$.[3] In thin films, $BiFeO_3$ is distorted by stresses associated with the epitaxial mismatch and signatures of monoclinic[4,5] and tetragonal[6] overall symmetries have been reported. No consensus for the crystallographic phases of $BiFeO_3$ thin films has yet been reached. An additional complication arises because $BiFeO_3$ thin films are often grown on miscut substrates, which promote epitaxy by modifying the kinetics of growth but cause the $BiFeO_3$ layer to be anisotropically strain.[7] Here we describe the mechanism of this relaxation and its effects on the overall symmetry of the $BiFeO_3$ thin film.

Our structural study includes both area-averaged laboratory source x-ray diffraction and synchrotron x-ray microdiffraction. Conventional millimeter-scale x-ray beams average over a large number of micron-scale mosaic blocks. As a result, the reciprocal-space resolution with which diffraction studies of the symmetry of $BiFeO_3$ thin films can be performed is reduced by the distribution of crystallographic directions arising from the large mosaic spread in partially relaxed thin films, typically 0.1° to 0.5°. Synchrotron x-ray microdiffraction, however, allows diffraction studies to be conducted with higher precision using individual mosaic blocks. Microdiffraction studies were conducted using 11.5 keV photons focused to a full-width-at-half-maximum (FWHM) of 110 nm using a Fresnel zone plate at station 2ID-D of the Advanced Photon Source. The 400 nm thick epitaxial $BiFeO_3$ (001) thin films were grown using off-axis sputtering on a 15 nm thick $SrRuO_3$ layer on a $SrTiO_3$ (001) substrate miscut by 4° toward [010].[8]

Reciprocal space maps of the $BiFeO_3$ (002) reflection, acquired with using a laboratory diffractometer, reveal the area-averaged orientation of the $BiFeO_3$ layer (Fig. 1). To acquire Fig. 1, the sample was oriented with the miscut direction in the scattering plane. The $SrRuO_3$ layer tilts *away* from the average surface due to expansion at substrate step edges and quantitatively agrees with the direction and value predicted by the Nagai model.[9] The $BiFeO_3$ is rotated *toward* the average sample surface normal by 0.13° with respect to $SrRuO_3$ and by a total of 0.073° with respect to the $SrTiO_3$

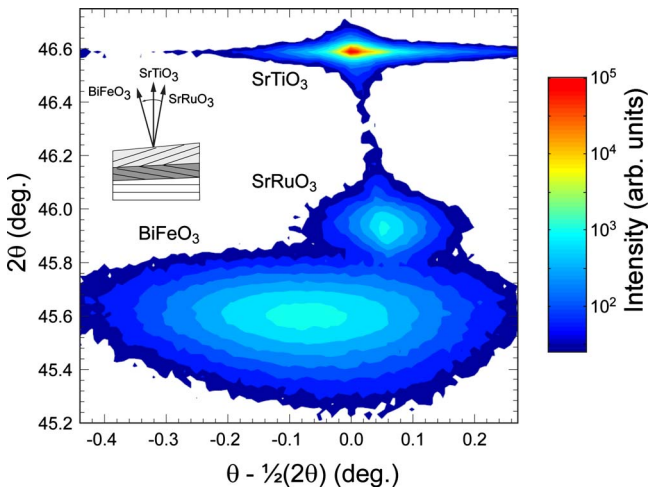

FIG. 1. (Color online) Area-averaged reciprocal space map of the (002) reflections of $BiFeO_3$, $SrTiO_3$, and $SrRuO_3$. The $SrRuO_3$ reflection is rotated by 0.057° from the substrate reflection away from the sample surface. The $BiFeO_3$ (002) is rotated in the opposite direction by 0.073° from the substrate, a total of 0.13° from the underlying $SrRuO_3$ film. The inset shows the orientations of the $BiFeO_3$, $SrRuO_3$, and $SrTiO_3$ (002) planes.

a)Present address: Department of Physics and Engineering Physics, University of Tulsa, Tulsa, Oklahoma USA.
b)Electronic mail: evans@engr.wisc.edu.

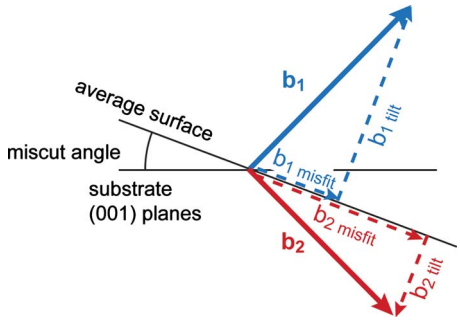

FIG. 2. (Color online) Components of dislocations relaxing an epitaxial thin film on a miscut substrate, after Mooney *et al.*, Ref. 10. The Burgers vectors $\mathbf{b}_1$ and $\mathbf{b}_2$ can be decomposed into $\mathbf{b}_{misfit}$ and $\mathbf{b}_{tilt}$. The component $\mathbf{b}_{misfit}$ results from the projection of the Burgers vector onto the epitaxial stress applied to the film and is the component which relaxes the film. $\mathbf{b}_{tilt}$ rotates the (001) planes of the film. The misfit component of $\mathbf{b}_2$ is larger than that of $\mathbf{b}_1$, so that dislocations with Burgers vector $\mathbf{b}_2$ are preferentially nucleated.

substrate, as depicted schematically in Fig. 1. Rotation toward the surface normal does not agree with the Nagai model, even qualitatively. The azimuthal dependence of these angles shows that the maximum rotation of the $BiFeO_3$ layer occurs in the plane including the miscut direction and the surface normal. This rotation has previously been observed in similar films by Jang *et al.*[8] and here we describe the specific relaxation mechanism leading to this effect.

The rotation of the $BiFeO_3$ results from preferential nucleation of dislocations in response to shear stresses, an effect that was discovered in epitaxial SiGe on miscut Si (001).[10] SiGe relaxes by a mechanism in which dislocation loops nucleate at the surface and propagate through the film thickness, leaving one edge of the loop at the substrate-film interface.[11,12] The relevant Burgers vector for SiGe are in the 1/2[101] family which glide on a {111} plane.[11] Two of the Burgers vectors that can relax a compressively strained film are labeled $\mathbf{b}_1$ and $\mathbf{b}_2$ in Fig. 2. Each has a misfit component $\mathbf{b}_{misfit}$, relaxing shear stress in the film, and a component $\mathbf{b}_{tilt}$ that rotates (001) planes. On a miscut substrate, there is a larger resolved shear stress on one of the two slip systems because the stress lies in the plane of the average surface rather than in the (001) plane. Dislocations with the larger resolved stress have lower activation energy for nucleation and are thus preferentially nucleated. Tilt components of the preferred slip system for the compressively strained $BiFeO_3$ on $SrTiO_3$ system, $\mathbf{b}_2$ in Fig. 2, rotate $BiFeO_3$ toward the average surface normal. The situation would be reversed for films under tensile stress, leading to rotations in the opposite direction.

The dislocations necessary for the relaxation mechanism of Ref. 10 have been observed in epitaxial perovskite thin films.[13,14] A full dislocation with Burgers vectors in the ⟨101⟩ family can dissociate into two partial dislocations at the substrate-film interface, so that 1/2 $[10\bar{1}]$ dissociates into 1/2 [100] and 1/2 $[00\bar{1}]$. The $[00\bar{1}]$ component produces the tilt familiar from the SiGe system. Preferential nucleation on a miscut substrate leads to an overall tilt toward the surface normal in compressively strained films, in agreement with experimental observations. Dislocations with slip systems along the direction of the miscut also face higher activation barriers, and the stress along the directions of the steps is thus more slowly relaxed than the stress along the miscut direction.

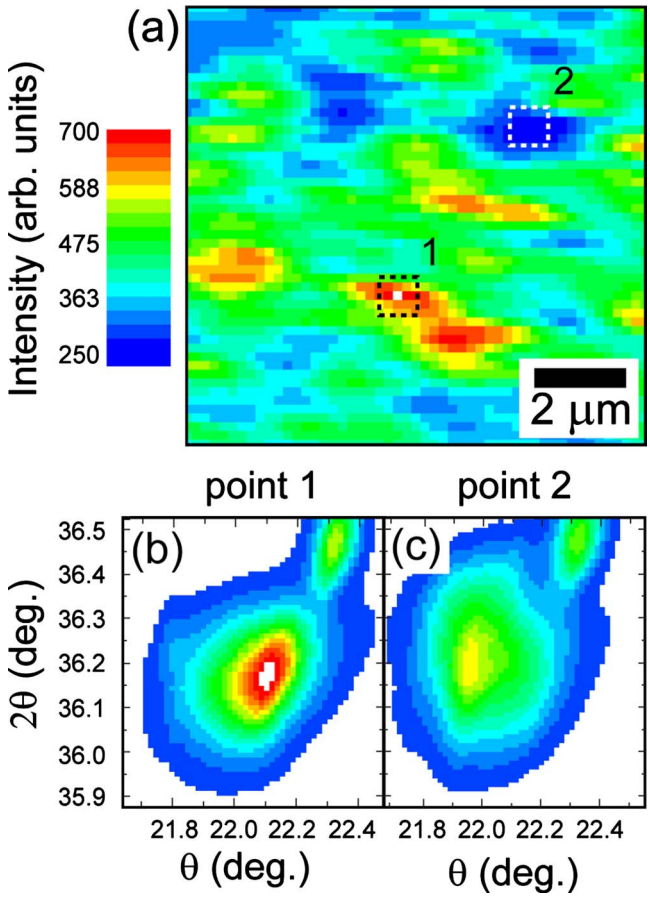

FIG. 3. (Color online) (a) X-ray microdiffraction image of mosaic blocks using the (002) reflection of $BiFeO_3$, acquired with diffractometer angles given at the maximum intensity in the area marked 1. (b), (c) Reciprocal space maps taken at positions 1 and 2 on the surface.

X-ray microdiffraction was used to probe the crystallographic structure within individual mosaic blocks within the $BiFeO_3$ film. Images of the mosaic blocks were acquired by plotting the intensity of the $BiFeO_3$ (002) reflection as a function of position of the x-ray beam on the sample. Individual mosaic blocks appear in Fig. 3(a) as contiguous areas of uniform intensity the order of 1 μm in extent. The structural relationship among mosaic blocks can be determined using diffraction patterns acquired at a series of positions on the sample. Reciprocal space maps acquired in the high- and low-intensity regions of Fig. 3(a) appear in Figs. 3(b) and 3(c). These two blocks produce $BiFeO_3$ reflections that are separated by a 0.15° rotation, well within the 0.3° FWHM of the area-averaged $BiFeO_3$ (002) peak in Fig. 1. The reciprocal space maps in Figs. 3(b) and 3(c) do not exhibit any splitting of the (002) reflection, even at the higher resolution afforded by the local probe. Each mosaic block thus consists of a single crystal or a series of crystals sharing a common set of (001) planes.

Further structural information can be obtained using reflections that are sensitive to the difference between ferroelectric domains. A map of diffracted intensity from the $BiFeO_3$ {103} reflections appears in Fig. 4(a). This map reveals a mosaic block structure qualitatively similar to the map obtained using the (002) reflection. The {103} reflection however, is sensitive to the structural difference between ferroelectric domains within individual mosaic blocks. Figures 4(b) and 4(c) are reciprocal space maps taken at points 1

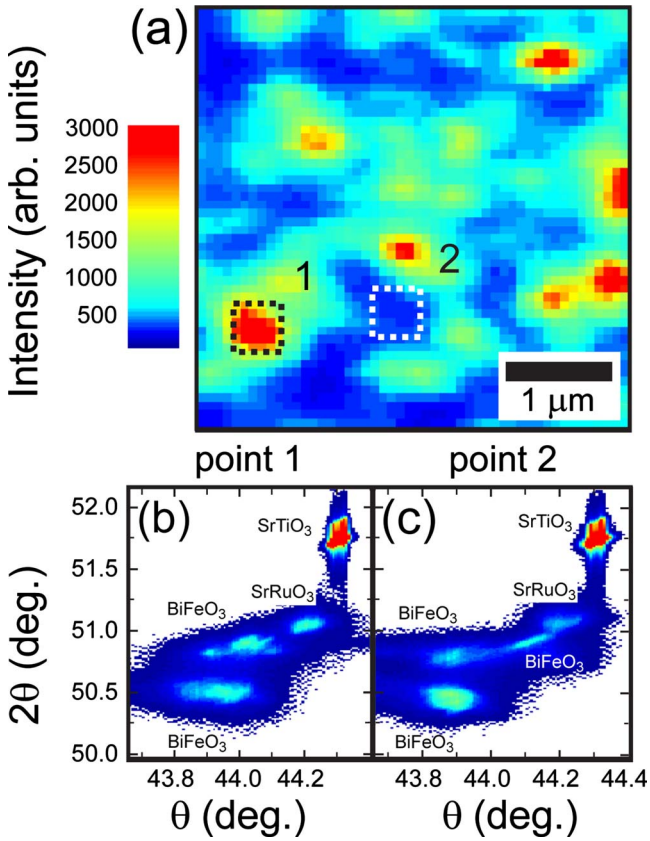

FIG. 4. (Color online) Microdiffraction image using the $BiFeO_3$ {103} reflections at $2\theta=50.73°$ at the area marked 1. Reciprocal space maps taken at positions 1 (b) and 2 (c) on the surface. There are at least two $BiFeO_3$ {103} reflections, arising from the presence of multiple polarization domains within each mosaic block.

and 2 of Fig. 4(a). In comparison with the unsplit (002) reflections, each mosaic block exhibits multiple {103} reflections.

The pseudocubic {103} of $BiFeO_3$ reflections are split by the rhombohedral distortion of the unit cell, leading to two distinct *d*-spacings and producing the x-ray reflections near 50.5° and 51.0° in Figs. 4(b) and 4(c). The existence of multiple {103} reflections within the volume probed by the focused x-ray beam indicates that the scattering volume encompasses more than one polarization domain. The reflections in Figs. 4(b) and 4(c) are consistent with a striped polarization domain structure in which the in-plane component of the polarization of neighboring domains forms a 90° angle. This 71° domain configuration is a common motif in rhombohedral films on cubic substrates.[15]

The reciprocal space location of the {103} reflections in Figs. 4(b) and 4(c) depends not only on crystallographic phase of the $BiFeO_3$ thin film but also on the orientation of each domain and on the stress field acting on it. The stress is complicated and highly anisotropic with respect to the substrate as a result of the anisotropy of the dislocation-mediated relaxation mechanism. The domain structure induces a further distortion. The $BiFeO_3$ {103} reflections are broad in reciprocal space due to the wide range of stresses acting on each domain. The two domain directions within the stripe pattern have different crystallographic orientations and are thus distorted differently by the stress field. The overall symmetry of the $BiFeO_3$ thin film is extremely low because of these effects, regardless of the symmetry of the starting phase. The many previous observations of symmetries other than rhombohedral in $BiFeO_3$ thin films[4–6] can largely be explained by the anisotropic stress imposed on a rhombohedral crystal by relaxation.

The anisotropic epitaxial relaxation of $BiFeO_3$ films on miscut $SrTiO_3$ substrates can be generalized to perovskite materials grown on substrates with lower symmetry than $SrTiO_3$, such as orthorhombic $DyScO_3$ or $NdGaO_3$. These substrates have a nonsquare surface unit cell, leading to anisotropic stress in pseudocubic epitaxial films and to a competition between multiple mechanisms for anisotropic relaxation. A nonmiscut orthorhombic substrate, for example, would cause a thin film to relax preferentially along the axis with larger lattice mismatch, but would not produce a net tilt of the film. Introducing a miscut to the orthorhombic substrate would further lower the symmetry of the applied stress and cause the film to tilt either toward the average surface for a compressively strained film or away from the average surface for a tensile strained film. Structural anisotropy controlled in this way will affect the electromechanical properties and the preferred orientations of magnetic moments, and can in principle be used as an additional degree of freedom influence the performance of complex oxide devices.

This work was supported by the National Science Foundation under Grant No. DMR-0705370. Use of the Advanced Photon Source was supported by the U.S. Department of Energy, Office of Science, Office of Basic Energy Sciences, under Contract No. W-31-109-Eng-38. C.B.E. acknowledges the financial support of the National Science Foundation through Grant No. ECCS-0708759 and the Office of Naval Research through Grant No. N00014-07-1-0215.

[1]C. Ederer and N. A. Spaldin, Phys. Rev. B **71**, 060401 (2005).
[2]S. Hong, J. A. Klug, M. Park, A. Imre, M. J. Bedzyk, K. No, A. Petford-Long, and O. Auciello, J. Appl. Phys. **105**, 061619 (2009).
[3]F. Kubel and H. Schmid, Acta Crystallogr., Sect. B: Struct. Sci. **46**, 698 (1990).
[4]J. Wang, J. B. Neaton, H. Zheng, V. Nagarajan, S. B. Ogale, B. Liu, D. Viehland, V. Vaithyanathan, D. G. Schlom, U. V. Waghmare, N. A. Spaldin, K. M. Rabe, M. Wuttig, and R. Ramesh, Science **299**, 1719 (2003).
[5]G. Xu, J. Li, and D. Viehland, Appl. Phys. Lett. **89**, 222901 (2006).
[6]S. Geprägs, M. Opel, S. T. B. Goennenwein, and R. Gross, Philos. Mag. Lett. **87**, 141 (2007).
[7]J. E. Ayers and S. K. Ghandhi, J. Cryst. Growth **113**, 430 (1991).
[8]H. W. Jang, D. Ortiz, S. H. Baek, C. M. Folkman, R. R. Das, P. Shafer, Y. Chen, C. T. Nelson, X. Pan, R. Ramesh, and C. B. Eom, Adv. Mater. **21**, 817 (2009).
[9]H. Nagai, J. Appl. Phys. **43**, 4254 (1972).
[10]P. Mooney, F. K. LeGoues, J. Tersoff, and J. O. Chu, J. Appl. Phys. **75**, 3968 (1994).
[11]M. A. Capano, Phys. Rev. B **45**, 11768 (1992).
[12]C. J. Gibbings, C. G. Tuppen, and M. Hockly, Appl. Phys. Lett. **54**, 148 (1989).
[13]T. Suzuki, Y. Nishi, and M. Fujimoto, Philos. Mag. A **79**, 2461 (1999).
[14]S. Stemmer, S. K. Streiffer, F. Ernst, and M. Rühle, Phys. Status Solidi A **147**, 135 (1995).
[15]S. K. Streiffer, C. B. Parker, A. E. Romanov, M. J. Lefevre, L. Zhao, J. S. Speck, W. Pompe, C. M. Foster, and G. R. Bai, J. Appl. Phys. **83**, 2742 (1998).